

# Dynamics of a dust grain in a system with albedo, radiation under variable accumulations and masses

## Abstract

In this paper, we have deduced the dynamical differential equations of a dust grain in a system with albedo, radiation pressure under effects of variable accumulations of material points and masses. The system consists of a dust grain passively gravitating in the field of two bodies whose masses are changing with time and the three bodies are enclosed by a variable mass accumulation of material points. The analysis considers the bigger body as a radiation source while the smaller one is an albedo body. Further, the masses of the main bodies and the accumulations change over time according to the Mestschersky Unified Law (MUL), while the motion of the main bodies is governed by the Gylden-Mestschersky equation. It is observed that the equations of motion of this problem differ from the restricted three-body problem with variable masses due to the influence of the radiation, albedo factors and the varying mass of the accumulations around the bodies. Additionally, to derive the relation that connects the albedo and radiation pressure, we assume that the luminosities and radius of both bodies vary and we introduced a transformation to describe it. Finally, the model is applied to three systems, which are: Proxima-Centauri-Dust disk, Sun-Mars-Asteroid belt and Sun-Saturn-Kuiper belt. The time series, surface and contour plots are presented to demonstrate the impacts of the model parameters on the dynamics of the dust grain. This study can be instrumental in mission design for space exploration and also aid in understanding the stability of celestial bodies like asteroid motion near the Lagrange points of the systems.

**Keywords:** R3BP, Variable Masses, Accumulation, Albedo, Radiation Pressure

Volume 9 Issue 2 - 2025

Leke Oni,<sup>1</sup> Veronica Ugbedeoj Cyril-Okeme,<sup>2</sup> Jessica Gyegwe<sup>2</sup>

<sup>1</sup>Department of Mathematics, College of Science, Joseph Sarwuan Tarka University, Nigeria

<sup>2</sup>Department of Mathematics, Faculty of Science, Federal University Lokoja, Nigeria

**Correspondence:** Leke Oni, Department of Mathematics, College of Science, Joseph Sarwuan Tarka University, P.M.B 2373 Benue-State, Nigeria

**Received:** February 5, 2025 | **Published:** May 12, 2025

## Introduction

The restricted three-body problem (R3BP) addresses the motion of a small, infinitesimal mass under the gravitational influence of two larger bodies, known as primaries, which move in circular orbits around their shared center of mass due to mutual gravitational attraction. The small mass does not affect the motion of the primaries. Since no general solution exists for the circular restricted three-body problem (CR3BP), particular solutions, known as Lagrangian or equilibrium points (EPs), are typically sought. In the classical R3BP, there are five such points: two triangular and three collinear. Euler<sup>1</sup> identified the three collinear points, and Lagrange<sup>2</sup> discovered the triangular ones. Over time, the R3BP has been studied from multiple perspectives, with researchers examining the effects of various parameters on the orbits of the primaries and the third body. These studies have included the introduction of perturbing forces, such as Coriolis and centrifugal forces, radiation pressure, and the gravitational influence of a disk, as well as variations where the motion of the third body is restricted to one of the primaries. Additionally, investigations have focused on cases where one, two, or all of the masses vary with time.

The classical R3BP assumes that the masses of celestial bodies remain constant, but observations of isotropic radiation and mass absorption in stars led scientists to extend the problem to cases with variable masses. This is especially relevant in double star systems, where mass changes occur more rapidly. Examples include rocket motion, black hole formation, satellite orbits around radiating stars surrounded by clouds of varying mass, and comets losing mass due to interactions with the solar wind. The study of astronomical objects with variable mass has broad applications in stellar, galactic, and planetary dynamics.

The two-body problem with variable mass entered scientific literature with the work of Gylden,<sup>3</sup> who modeled the relative motion

of two mass points under mutual gravitational attraction, where the sum of their masses varied with time. Mestschersky<sup>4,5</sup> further generalized the problem by showing that Gylden's model was a special case where the masses vary isotropically, leading to what is now called the Gylden-Mestschersky problem (GMP).

Bekov<sup>6</sup> was the first to discover the coplanar EPs  $L_6$  and  $L_7$  with variable mass, expanding on Gelf'gat's<sup>7</sup> work. These points are located outside the plane of the primary bodies' revolution. Luk'yanov<sup>8</sup> further investigated a similar formulation, finding four additional coplanar solutions and explored the potential existence of infinitely distant solutions,  $L_{\pm\infty}$ . In 1990, Luk'yanov<sup>9</sup> studied the stability of EPs in the R3BP with variable primary masses governed by the Mestschersky Unified Law (MUL) and confirmed that all EPs (collinear, triangular, and coplanar) were stable with respect to the Mestschersky coordinate system.

Singh and Leke<sup>10-12</sup> examined under different characterizations the motion and stability of EPs in the restricted problem with varying primary masses following the MUL and governed by the GMP. Veras et al.<sup>13</sup> studied the effect of isotropic mass variation in planetary systems, exploring the potential ejection of planets. Letelier and Da Silva<sup>14</sup> analyzed particular solutions in the R3BP where bodies gain or lose mass from a static atmosphere, finding solutions analogous to the five stationary points of the constant-mass R3BP, with the relative distances between bodies changing over time. Additionally, they identified coplanar, infinitely distant, and ring solutions. Leke and Singh<sup>15</sup> examined the out-of-plane equilibrium points of extrasolar planets in the field of two central binaries with variable masses while Leke and Mmaju<sup>16</sup> explored the zero velocity curves of a dust grain around equilibrium points under effects of radiation, perturbations and variable mass Kruger 60. Recently, Leke, et al.<sup>17-19</sup> investigated the impact of triaxiality on motion around triangular points and unveiled

motion around out-of plane EPs of the R3BP with variable shape, respectively.

The R3BP in the case of constant masses have carried out studies where one of the primaries is a light source while the other is a sink source, which is referred to as albedo. Albedo can be defined as the fraction of incident solar radiation returned to space from the surface of the planet and is one of the most interesting non-gravitational force having effects on the motion of an infinitesimal particle.

Idrisi<sup>20</sup> investigated the existence and stability of the CR3BP under the effect of albedo when the smaller primary is an ellipsoid, while Idrisi and Ullah<sup>21</sup> examined effects of albedo on the existence and stability of EPs when the smaller primary is a homogenous ellipsoid. Further, Idrisi and Ullah<sup>22</sup> studied the non-linear libration points in the elliptic R3BP with effects of oblateness and albedo of the smaller primary in the Sun-Earth system and found that the non-linear libration points form an isosceles triangle with the primaries and any increase of eccentricity cause the libration points to move vertically downward.

Researches on planetary systems have revealed the presence of accumulations of material points which could be dust particle disks, debris disk, asteroid belts or Kuiper belt around bodies in our stellar or solar systems. These accumulations significantly impact the orbital elements of planets, particularly in circularizing orbits, and play a role in planet-belt interactions within planetary systems. The investigations of motion and periodic orbits in R3BP with inclusion of an accumulation of material points have been carried out by Singh and Taura,<sup>23</sup> Singh and Leke,<sup>24,25</sup> Jiang and Yeh<sup>26</sup> and, Yeh and Jiang,<sup>27</sup> under different modifications.

Motivated by the vast applications of the R3BP, our aim in this paper is to deduce the dynamical equations of a dust grain in a system using the model of the R3BP and assuming that the bigger primary is a radiating body, while the smaller is an albedo type when the configuration is surrounded by an accumulation of material points. The model is applied to three systems, which are: Proxima-Centauri-dust disk, Sun-Mars-Asteroid belt and Sun-Saturn-Kuiper belt. Here, Proxima and Centauri are the bigger and smaller body in the stellar system while the dust disk is the accumulation. Also, the Sun and Mars, and, Sun and Saturn are the main bodies in our solar system while the asteroid and Kuiper belts are the accumulations, respectively.

Therefore this paper is alienated into 4 sections: Sect. 1 conveys the introduction while Sect. 2 entails the dynamical derivations of the problem, Sects. 3 and 4 respectively deals with the numerical illustrations and discussion while the conclusion is given in Sect.5

## Dynamical equations

In this problem, we extend the model given by Taura and Leke<sup>28</sup> by assuming that the first primary is a source of radiation and the second one is an albedo body. The problem is applied to three systems in which the bigger primary is a radiating body, the smaller is an albedo body and both are enclosed by an accumulation of material points.

## Equation of motion of two- body with variable masses

The two-body problem (2BP) is the starting point for nearly all reference books in the field of astrodynamics. The basic problem describes the motion of two point-masses in mutual gravitational attraction, and is given by

$$\frac{d\vec{v}}{dt} = \frac{\mu}{r^2} \frac{\vec{r}}{r} \quad (1)$$

where  $\vec{v}$  is the velocity,  $\mu$  is the product of the gravitational constant  $G$  and the sum of the masses, and  $\vec{r}$  is the distance between

the stars

$$r^2 \dot{\theta} = C \quad (2)$$

Equation (2) is the area integral of the system,  $\theta$  is the angular velocity of revolution of the bodies of masses  $m_1$  and  $m_2$ , and  $C$  is the constant of integration

Now, the problem of two bodies with variable masses, which is an analogy of the classical problem of two bodies with constant masses, one understands the problem of motion of two primary bodies, the masses  $m_1$  and  $m_2$  of which vary with time under certain laws and between which only the gravitational force acts. In this premise, the relative motion of the problem of two bodies with variable masses is described by the equation

$$\ddot{\vec{r}} = -G \frac{(m_1 + m_2)}{r^3} \vec{r} \quad (3)$$

Equation (3) is analogous to equation (1) of the classical problem of two bodies with constant masses, with the difference that now; the sum of the masses is a certain function of time. This equation is called the Gylden-Mestschersky problem (GMP).

Mestschersky (1902), reduced the GMP through the introduction of new variables and time to the equations of the classical problem of two bodies with constant masses by a transformation, which was thereafter known as the Mestschersky (1902) transformation (MT) and is given by

$$\begin{aligned} x &= \xi R(t), y = \eta R(t), z = \zeta R(t), \frac{dt}{d\tau} = R^2(t) \\ r_i &= \rho_i R(t), (i = 1, 2), r = \rho_{12} R(t) \end{aligned} \quad (4)$$

where  $R(t) = \sqrt{\alpha t^2 + 2\beta t + \gamma}$ ;  $\xi, \eta, \zeta, \tau$  are the new variables and  $\rho_{\mathbf{e}}$  is constant.

Further, Mestschersky<sup>29</sup> came up with a law in which he considered the masses and their sum to vary in the same proportion in such a way that

$$\mu(t) = \frac{\mu_0}{R(t)}, \mu_1(t) = \frac{\mu_0}{R(\mathbf{B})}, \mu_2(t) = \frac{\mu_0}{R(t)}$$

where  $\mu_1(t) = Gm_1(t)$ ,  $\mu_2(t) = Gm_2(t)$ ,  $\mu(t) = \mu_1(t) = \mu_2(t)$ ,  $\mu_{10}$  and  $\mu_{20}$  are constants.

Equation (5) is called the Mestschersky unified law (MUL) and it assures that the centre of the mass of the system moves initially, and

$$r\mu = \kappa C^2 \quad (6)$$

is the particular integral of the GMP where  $\kappa$  is a constant.

## Equations of motion of the third body

Let us consider a rotating frame of reference  $O_{xyz}$ , where O is the origin. We suppose that  $m_1$  and  $m_2$  are the masses of the massive bodies and  $m_3$  be the mass of the dust grain. We have taken the line joining  $m_1$  and  $m_2$  as the  $x$ -axis. The coordinates of  $m_1$  and  $m_2$  are  $(x_1, 0, 0)$  and  $(x_2, 0, 0)$  respectively, and that of the dust grain is  $(x, y, z)$ . Here we suppose that the masses of the bodies vary with respect to time with the consideration that the bigger body is a source of radiation while the smaller one is an albedo body. Let the radius vector from  $m_3$  to  $m_1$  be  $r_1$ ,  $m_3$  to  $m_2$  be  $r_2$  and the distance between the bodies be  $r$  and let  $\omega$  be the angular velocity.

Now, the kinetic energy of the dust grain in the rotating frame of reference  $O_{xyz}$  is given by

$$T = \frac{1}{2} m_3 (\dot{x}^2 + \dot{y}^2 + \dot{z}^2) + m_3 \omega (x\dot{y} - y\dot{x}) + \frac{1}{2} m_3 (x^2 + y^2) \omega^2 \quad (7)$$

while its potential energy, when the masses of the bodies and the accumulations vary with time is:

$$U = -Gm_3 \left[ \frac{m_1(t)q_1}{r_1} + \frac{m_2(t)q_A}{r_2} + \frac{M_d(t)}{\sqrt{\mathfrak{R}^2 + (a + \sqrt{b^2 + z^2})^2}} \right] \quad (8)$$

$$\text{where } r_1^2 = (x - x_1)^2 + y^2 + z^2, \quad r_2^2 = (x - x_2)^2 + y^2 + z^2$$

$r_1$  and  $r_2$  are time dependent distances of the dust grain from the bodies,  $q_1$  is the radiation factor of the bigger body,  $q_A$  is the albedo effect of the smaller one.  $M_d$ ,  $\mathfrak{R}$ ,  $a$  and  $b$  are the varying mass, radius, radial scale-length, and vertical scale-height, of the accumulation, respectively. The parameters  $a$  and  $b$  describes the kind of the density of the accumulation and by varying these parameters, the mass distribution can be modeled with a range of thickness.  $a$  is the flatness parameter and determines the flatness of the profile while  $b$  is the core parameter that defines the size of the core of the density profile,  $G$  is the gravitational constant and  $\mathfrak{R} = \sqrt{x^2 + y^2 + z^2}$ .

The relation that connects the albedo and radiation pressure is (Idrisi 2017; Idrisi & Ullah 2018)

$$\varepsilon_A = \varepsilon_1 \frac{m_1 L_{b2}}{m_2 L_{b1}} \quad (9)$$

where  $\varepsilon_1 = 1 - q_1 < 1$ ,  $\varepsilon_A = 1 - q_A < 1$  while  $L_{b1}$  and  $L_{b2}$  are the luminosity of the bigger and the smaller bodies, respectively and are assumed to vary with time as the masses of the bodies change with time.

Now let  $p_x, p_y$  and  $p_z$  be the generalized components of momentum then,

$$p_x = \frac{\partial T}{\partial \dot{x}} = m_3 (\dot{x} - \omega y), \quad p_y = \frac{\partial T}{\partial \dot{y}} = m_3 (\dot{y} + \omega x), \quad p_z = \frac{\partial T}{\partial \dot{z}} = m_3 \dot{z} \quad (10)$$

This implies

$$\dot{x} = \frac{p_x}{m_3} + \omega y, \quad \dot{y} = \frac{p_y}{m_3} - \omega x, \quad \dot{z} = \frac{p_z}{m_3} \quad (11)$$

Substituting equations of system (10) in (7) and simplifying, we at once have

$$T = \frac{1}{2m_3} (p_x^2 + p_y^2 + p_z^2)$$

Now, the Hamiltonian  $H$  is given by

$$H = \frac{1}{2} m_3 (\dot{x}^2 + \dot{y}^2 + \dot{z}^2) - \frac{1}{2} m_3 \omega^2 (x^2 + y^2) + U \quad (12)$$

Using system (10) in equation (11), we get

$$H = \frac{1}{2m_3} (p_x^2 + p_y^2 + p_z^2) + \omega (yp_x - xp_y) + U \quad (13)$$

Now, from the Hamiltonian canonical equations, we have

$$\dot{p}_x = -(\omega p_y) - \frac{\partial U}{\partial x}, \quad \dot{p}_y = -\omega p_x - \frac{\partial U}{\partial y}, \quad \dot{p}_z = -\frac{\partial U}{\partial z} \quad (14)$$

Since the main bodies move within the frameworks of the GMP and their masses vary with time as defined by the MUL, then  $p_x, p_y, p_z$  and the angular velocity  $\omega$  will all be time dependent. So, we differentiate system (10) w.r.t time and compare with equations (14), to get

$$m_3 (\dot{x} - \omega \dot{y} - \dot{\omega} y) = \omega p_y - \frac{\partial U}{\partial x}, \quad m_3 (\dot{y} + \omega \dot{x} - \dot{\omega} x) = -\omega p_x - \frac{\partial U}{\partial y}, \quad (15)$$

$$m_3 \dot{z} = -\frac{\partial U}{\partial z}$$

Substituting equations of system (11) in (15), we get

$$m_3 (\ddot{x} - \dot{\omega} \dot{y} - \dot{\omega} y) = \omega m_3 (\dot{y} + \omega x) - \frac{\partial U}{\partial x}, \quad m_3 (\ddot{y} - \dot{\omega} \dot{x} - \dot{\omega} x) = -\omega m_3 (\dot{x} - \omega y) - \frac{\partial U}{\partial y}, \quad (16)$$

$$m_3 \ddot{z} = -\frac{\partial U}{\partial z}$$

If we differentiate equation (8) w.r.t  $x, y$  and  $z$ , respectively, and substitute in (16) while multiplying the results throughout by  $\frac{1}{m_3}$ , we get

$$\ddot{x} - 2\dot{\omega} \dot{y} = \omega^2 x + \dot{\omega} y - \frac{\mu_1 q_1 (x - x_1)}{r_1^3} - \frac{\mu_2 q_A (x - x_2)}{r_2^3} - \frac{\mu_d x}{\left( \mathfrak{R}^2 + (a + \sqrt{z^2 + b^2})^2 \right)^{3/2}}$$

$$\ddot{y} + 2\dot{\omega} \dot{x} = \omega^2 y + \dot{\omega} x - \frac{\mu_1 q_1 y}{r_1^3} - \frac{\mu_2 q_A y}{r_2^3} - \frac{\mu_d y}{\left( \mathfrak{R}^2 + (a + \sqrt{z^2 + b^2})^2 \right)^{3/2}} \quad (17)$$

$$\ddot{z} = -\frac{\mu_1 q_1 z}{r_1^3} - \frac{\mu_2 q_A z}{r_2^3} - \frac{\mu_d z}{\left( \mathfrak{R}^2 + (a + \sqrt{z^2 + b^2})^2 \right)^{3/2}} \left( 1 + \frac{a + \sqrt{z^2 + b^2}}{\sqrt{z^2 + b^2}} \right)$$

$$\text{where } \omega^2(t) = \frac{\mu(t)}{\kappa} \left[ \frac{1}{r^3} + \frac{2\mu_d r_c}{\left\{ r_c^2 + (a + \sqrt{z^2 + b^2})^2 \right\}^{3/2}} \right] \quad (18)$$

$$\mu_d = GM_d(t) \quad (19)$$

These equations describe the motion of the dust grain particle in the gravitational field of the main bodies enclosed by an accumulation of material points when both bodies and accumulation experience mass variations while the bigger body is a radiation emitter and the smaller one is an albedo body.  $r_c$  is the time dependent radial distance of the dust grain and the masses vary in accordance with the MUL while motion of the bodies is described by the GMP.  $\kappa$  is the constant of the integral of the GMP;  $\mu_d(t)$  is the product of the gravitational constant and mass of the accumulation of material points  $M_d$ .

Equations (17-19) are different from those of Taura and Leke<sup>28</sup> because of the presence of the radiation parameter of the bigger body and albedo coefficient of the smaller body. They are also different from those of Singh and Leke<sup>10-12</sup> due to the different characterizations of the model. The results of Taura and Leke,<sup>28</sup> Luk'yanov,<sup>8</sup> Bekov,<sup>6</sup>

can all be recovered from our dynamical equations of motion. If we set  $q_1 = q_A = 1$ , we recover the dynamical system of Taura and Leke.<sup>28</sup> If we set  $q_1 = q_A = 1$  and  $\mu_d = 0$ , we at once recover the dynamical equations of Bekov<sup>6</sup> and Luk'yanov.<sup>8</sup>

Next, we transform system (17-19), to a system with constant coefficients using the MT (3); the MUL (5); the particular integral and solutions of the GMP (6). Hence, by the MUL and the MT, we have:<sup>16</sup>

$$\mu_d(t) = \frac{M_{0d}}{R(t)}, \quad \mathfrak{R} = \rho R(t), \quad r_c = \rho_c R(t), \quad a = a_0 R(t),$$

$$b = b_0 R(t) \quad (20)$$

where  $M_{0d}$ ,  $\rho$ ,  $\rho_c$ ,  $a_0$  and  $b_0$  are constants.

Consequently, we transform (17-19) from  $(x, y, z, t)$  to the autonomized form  $(\xi, \eta, \zeta)$  and choose units of measurements, to get

$$\xi'' - 2\omega_0 \eta' = \frac{\partial \Omega}{\partial \xi}, \quad \eta'' - 2\omega_0 \xi' = \frac{\partial \Omega}{\partial \eta}, \quad \zeta'' = \frac{\partial \Omega}{\partial \zeta} \quad (21)$$

where

$$\Omega = \frac{\hat{e}\omega_0^2}{2}(\xi^2 + \eta^2 + \zeta^2) - \frac{\omega_0^2 r^2}{2} + \frac{\hat{e}q_1(1-\nu)}{\rho_1} + \frac{\hat{e}q_A \nu}{\rho_2} + \frac{\hat{e}M_{0d}}{(\rho^2 + (a_0 + \sqrt{\zeta^2 + b_0^2})^2)^{3/2}}$$

$$(22)$$

$$\omega_0^2 = 1 + \frac{2\kappa M_{0d} \rho_c}{\left\{ \rho_c^2 + \left( a_0 + \sqrt{\zeta^2 + b_0^2} \right)^2 \right\}^{3/2}} \quad (23)$$

$$\rho_1 = \sqrt{(\xi + \nu)^2 + \eta^2 + \zeta^2}, \quad \rho_2 = \sqrt{(\xi + \nu - 1)^2 + \eta^2 + \zeta^2} \quad (24)$$

$$\rho_c^2 = 1 - \nu + \nu^2, \quad \rho^2 = \xi^2 + \eta^2 + \zeta^2 \quad (25)$$

$M_{0d}$  is the mass of the accumulation and  $\rho_c$  is the radial distance of the dust grain in the autonomized R3BP with constant coefficients.

Equations (21-25) are autonomized system of equations with constant coefficients and these equations are different from those of Singh and Leke<sup>10-12</sup> due to the different characterizations of the model. The results of Luk'yanov,<sup>8</sup> Bekov,<sup>6</sup> can all be recovered from our dynamical equations of motion. If we set  $q_1 = q_A = 1$ , we recover the dynamical system of Taura and Leke.<sup>28</sup> If we set  $q_1 = q_A = 1$  and  $M_{0d} = 0$ , we at once recover the dynamical equations of Bekov<sup>6</sup> and Luk'yanov.<sup>8</sup> The autonomized equations were not obtained in the work of Taura and Leke.<sup>28</sup>

Now from equation (9), since the luminosities and radius of the bodies change with time, we assume that they vary in such a way that

$$L_{b1} = L_0 R^2(t), \quad L_{b2} = L_0 R^2(t) \text{ and } R_{1,2}^* = \rho_{1,2}^* R(t) \quad (26)$$

respectively

Hence, equation (9) is cast to the form

$$\varepsilon_A = \varepsilon_1 \frac{\mu_{10} L_{02}}{\mu_{20} L_{01}} \quad (27)$$

which consequently reduces to

$$\varepsilon_A = \frac{\varepsilon_1(1-\nu)}{\nu} k_1 \quad (28)$$

where,  $k_1 = \frac{L_0}{L_0}$  is a constant

## Results

In this numerical application we consider motion of the dust grain particle in the neighborhood of three systems, namely i. Proxima-Centauri-dust disk, ii. Sun-Mars-Asteroid belt and iii. Sun-Saturn-Kuiper belt. In this premise, we adopt the data given by Yousef and Kishor<sup>30</sup> which are presented in Table 1 below.

**Table 1** Numerical estimates for the systems: Proxima-Centauri-Dust disk; Sun-Mars-Asteroid belt and Sun-Saturn-Kuiper belt

System	Mass Parameter $\nu$	Radiation factor $q_1$	Albedo Coefficients $q_A$	Mass of the Enclosure $M_{0d}$	$T$	$\rho_c$
Proxima Centauri& dust disk	0.000031	0.92	0.9992	$2.5 \times 10^{-7}$	0.11	8
Sun-Mar & Asteroid Belt	0.0000003	0.97	0.9997	$1.6 \times 10^{-9}$	0.11	0.8
Sun-Saturn & Kuiper Belt	0.000286	0.99	0.9999	$3.0 \times 10^{-7}$	0.11	4.7

Using the Stefan-Boltzmann law, the luminosities of the bodies in the autonomized system can be expressed as  $L_{01} = 4\pi\rho_1^2 \sigma T_{e1}^4$  and  $L_{02} = 4\pi\rho_2^2 \sigma T_{e2}^4$ .<sup>30</sup> Here,  $\rho_{1,2}^*$  and  $T_{e1,e2}$  are the radius and effective temperature of the bigger and smaller body, respectively, for the autonomized system while  $\sigma$  is the Stefan-Boltzmann constant and  $\varepsilon$  is the emissivity of the smaller body.

Next, following Del Genio, et al.,<sup>31</sup> we introduce the albedo of the smaller body by rewriting luminosity  $L_q$  in terms of predicted albedo  $A^p$ :

$$L_{02} = \pi\rho_2^2 \sigma \varepsilon S_0 (1 - A^p) \quad (29)$$

where  $S_0$  is a solar constant.

Therefore, equation (28) can be represented as

$$q_A = 1 - \frac{(1-\nu)}{\nu} (1 - q_1) k_1 \quad (30)$$

$$\text{where } k_1 = \frac{\rho_2^2 \varepsilon S_0 (1 - A^p)}{4\rho_1^2 \sigma T_{e1}^4} \in (0,1) \quad (31)$$

where  $0 < q_1 \leq 1$  and  $q_1 < q_A \leq 1$  and  $A^p$  lies between 0 (if all incident radiations are absorbed) and 1 (if all incident radiations are reflected). Also, the value of  $k_1$  depends on the system in question.

Next, using the Mathematica software, we use a built-in adaptive solver NDSolve to solve equations (21) numerically and further plot the graphs of these solutions for the three systems in Fig 1 to 7 for different values of the mass variation parameter.

Next, we draw the 3D surface and contour plots of the solutions of equation (21), when motion takes place in the in-plane rotating system, for the Proxima-Centauri-Disk, Sun-Mars-Asteroid belt and Sun-Saturn-Kuiper belt systems, in Figure 8-10, respectively.



## Discussion

The dynamical equations of motion (17 and 21) of the R3BP with first primary radiating, second albedo primary, variable masses and disk has been deduced under the condition that the masses of the primaries vary in accordance with the GMP and their motion occur according to the MUL. Hence, with the assistance of the potential (8) and the Hamiltonian equations, the dynamical equations of motion of the R3BP with first radiating primary, second albedo primary, variable masses and accumulation of material points have been derived. These dynamical equations are not the same with those of Taura and Leke<sup>28</sup> due to the inclusion of radiating first primary and albedo second primary. Putting  $q_1 = q_A = 1$  equations (17) fully corresponds to those of Taura and Leke.<sup>28</sup> The luminosities and the radius of the primaries are assumed to also change with time as the mass variation process of the primaries takes place. Hence, following the MUL, we introduced a transformation for the luminosities and radius of the bodies which we now used to deduced the relation that connects the albedo of the smaller body and the radiation of the bigger body. Finally, we explored the dynamical equations of the autonomized system derived in equations (21) and sought for the numerical solutions when motion of the dust grain in the vicinity of the main bodies takes place in the in-plane rotating coordinates. Hence, our numerical illustrations took into account motion of a dust grain in the gravitational environments of three systems, namely Proxima-Centauri-Disk, Sun-Mars-Asteroid belt and Sun-Saturn-Kuiper belt. The time series plots of the solutions were presented for increasing mass variation parameter. Further, the surface and contour plots were given.

The plots drawn in Figure 1 to 7 are time series data of two state variables  $\xi(\tau)$  and  $\eta(\tau)$  from the numerical solutions of equations (21). The plot of  $\xi(\tau)$  and  $\eta(\tau)$  versus time, provides information about the trajectory of the dust grain over time under the gravitational influence of the systems. This enables us to study the system's stability or chaotic nature. It is seen that when the mass variation constant is in the interval  $0 < \kappa \leq 0.1$ , Figure 1&2 shows that the solutions are linear. However, as the mass variation parameter increases, it is observed from Figure 3a and Figure 3b, the solutions become oscillatory for the Proxima-Centauri-Disk and Sun-Mars-Asteroid belt systems but linear for the Sun-Saturn-Kuiper belt system. Further, as the bodies and the accumulations around them gain more mass, the solutions are oscillatory and in this case the oscillations in  $\xi(\tau)$  and  $\eta(\tau)$  are not due to the gravitational pull from the two larger masses, as it is the case in the classical R3BP, but due to the mass variation parameter, causing the dust grain to move in a periodic or quasi-periodic path. A spiraling trajectory suggests the dust grain is moving away or toward a stable configuration.

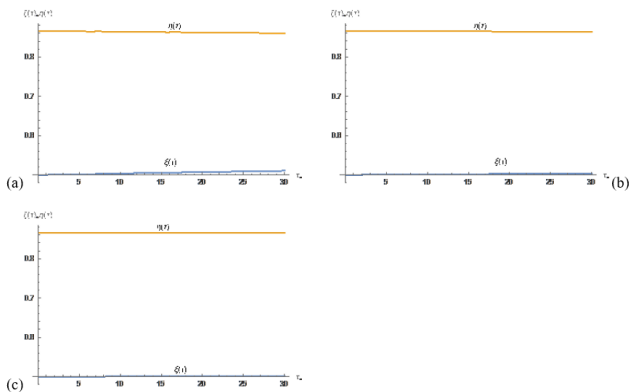


**Figure 1** Numerical solutions of equations (21) for (a) Proxima-Centauri-Disk (b) Sun-Mars-Asteroid belt and (c) Sun-Saturn-Kuiper belt system when  $\kappa = 0.0$ .

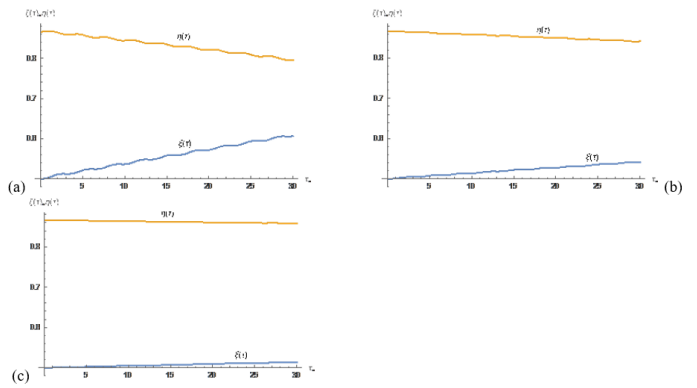


**Figure 2** Numerical solutions of equations (21) for (a) Proxima-Centauri-Disk (b) Sun-Mars-Asteroid belt and (c) Sun-Saturn-Kuiper belt system when  $\kappa = 0.1$ .

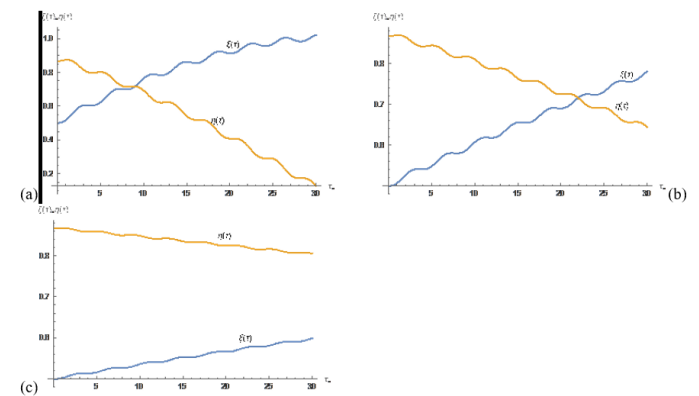


**Figure 3** Numerical solutions of equations (21) for (a) Proxima-Centauri-Disk (b) Sun-Mars-Asteroid belt and (c) Sun-Saturn-Kuiper belt system when  $\kappa = 0.5$ .

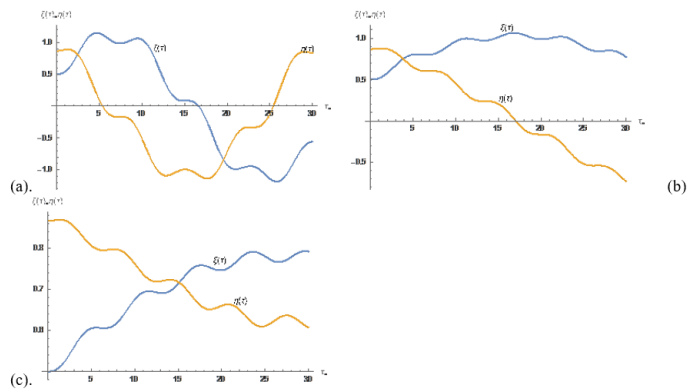


**Figure 4** Numerical solutions of equations (21) for (a) Proxima-Centauri-Disk (b) Sun-Mars-Asteroid belt and (c) Sun-Saturn-Kuiper belt system when  $\kappa = 1$ .

Figures 8-10 are the surface and contour plots of the dust grain in the gravitational environments of the Proxima-Centauri-Disk, Sun-Mars-Asteroid belt and Sun-Saturn-Kuiper belt systems, respectively, when the mass variation parameters are 0.001 and 2. The height of the surface plot represents the potential given in equation (21) and defined by the mass variation parameter, the radiation and albedo factors, the mass parameter and the mass of the accumulations around the systems. The valleys and peaks correspond to areas of low and high potential, respectively, influencing the possible trajectories and stability of the motion of the dust grain in the gravitational field of

the three systems. In the case of the contour plots, the mass variation parameter admits the difference in contour distribution. This is due to increasing mass of the primaries and the accumulations. The concentric nature of the contours represent regions of constant energy, which helps to understand the dynamics of the dust grain moving in the gravitational field of the three systems.

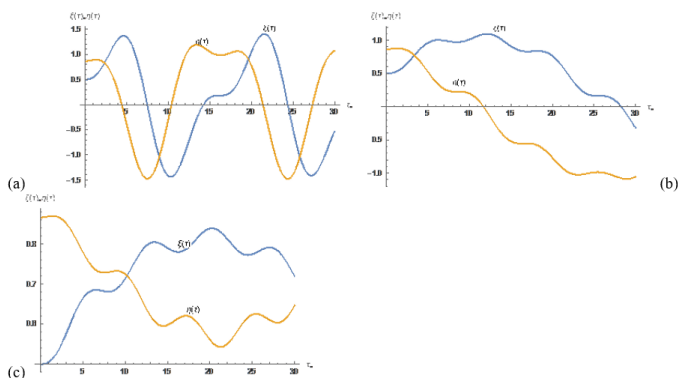


**Figure 5** Numerical solutions of equations (21) for (a) Proxima-Centauri-Disk (b) Sun-Mars-Asteroid belt and (c) Sun-Saturn-Kuiper belt system when  $\kappa = 1.0$ .

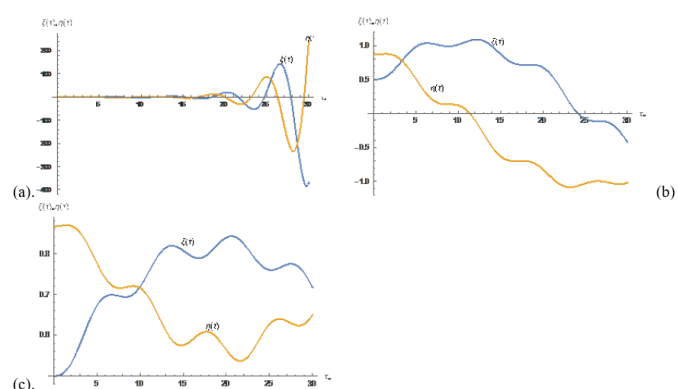


**Figure 6** Numerical solutions of equations (21) for (a) Proxima-Centauri-Disk (b) Sun-Mars-Asteroid belt and (c) Sun-Saturn-Kuiper belt system when  $\kappa = 1.1$ .

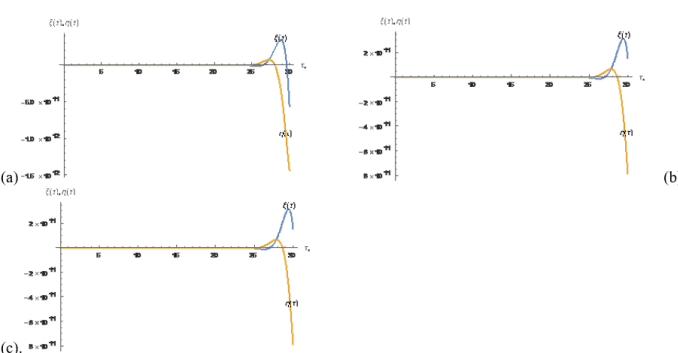


**Figure 7** Numerical solutions of equations (21) for (a) Proxima-Centauri-Disk (b) Sun-Mars-Asteroid belt and (c) Sun-Saturn-Kuiper belt system when  $\kappa = 2$ .

This study is vital in mission design for space exploration, particularly for finding stable orbits or transfer paths near planets or in binary systems, and it also aid in understanding the stability of natural systems like asteroid motion near the Lagrange points of Mars.

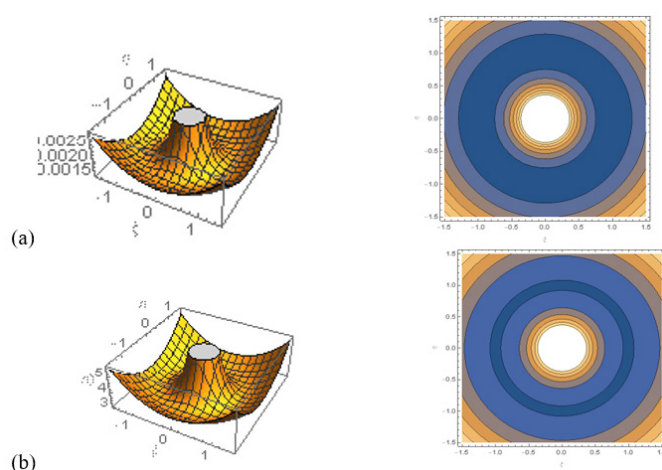


**Figure 8** 3D surface and contour plots of in-plane solutions of Proxima-Centauri-Disk system when (a)  $\kappa = 0.001$  (b)  $\kappa = 2$ .

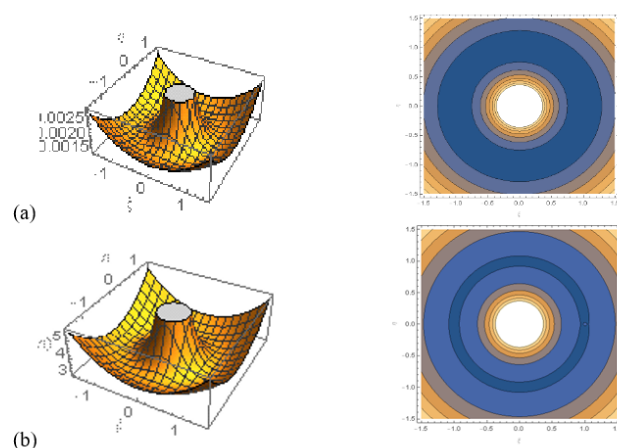


**Figure 9** 3D surface and contour plots of in-plane solutions of Sun-Mars-Asteroid belt system when  $\kappa = 0.001$  (b)  $\kappa = 2$ .

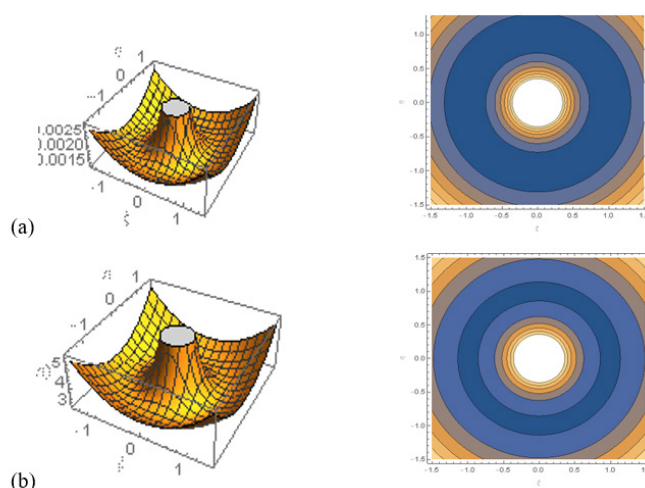


**Figure 10** 3D surface and contour plots of in-plane solutions of Sun-Saturn-Kuiper belt system when (a)  $\kappa = 0.001$  (b)  $\kappa = 2$ .

## Conclusion

This paper deduced the dynamical equations of a dust grain in a system with albedo, radiation pressure under effects of variable accumulations of material points and masses. The system is made up of a passively gravitating dust grain in the field of two bodies whose masses are assumed to be changing with time and the three bodies are enclosed by a variable mass accumulation of material points. The analysis assumed the bigger body as a radiation source while the smaller one is an albedo body. Further, the masses of the main bodies and the accumulations change with time according to the Mestschersky Unified Law (MUL), while the motion of the main bodies is governed by the Gylden-Mestschersky problem. It was observed that the equations of motion of this problem differed from the restricted three-body problem with variable masses due to the influence of the radiation, albedo factors and the varying mass of the accumulations around the bodies. The model was applied to three systems, which are: Proxima-Centauri-dust disk, Sun-Mars-Asteroid belt and Sun-Saturn-Kuiper belt. The time series, 3D surface and contour plots are presented to demonstrate the impacts of the model parameters on the dynamics of the dust grain.

## References

- Euler L. The motion in the rectilinear three-body problem. In: Szebehely V, ed. *Theory of Orbits*. Academic Press; 1967:144–149.
- Lagrange JL. *Collected Works*. Vol VI. Paris; 1873:229.
- Gylden H. Die Bahnbewegungen in einem Systeme von zwei Körpern in dem Falle, dass die Massen Veränderungen unterworfen sind. *Astron Nachr*. 1884;109:1–6.
- Mestschersky IV. Special cases of the Gylden Problems (A. N. 2593). *Astron Nachr*. 1893;132:129–130.
- Mestschersky IV. Ueber die Integration der Bewegungsgleichungen im Probleme zweier Körper von veränderlicher Masse. *Astron Nachr*. 1902;159:229–242.
- Bekov AA. Libration points of the restricted problem of three bodies with variable mass. *Sov Astron J*. 1988;33:92–95.
- Gelf'gat BE. *Current Problems of Celestial Mechanics and Astrodynamics*. Nauka; 1973.
- Luk'yanov LG. Particular solutions in the restricted problem of three bodies with variable masses. *Astron J Acad Sci USSR*. 1989;66:180–187.
- Luk'yanov LG. The stability of the libration points in the restricted three-body problem with variable masses. *Astron Zh*. 1990;67:167–172.
- Singh J, Leke O. Stability of the photogravitational restricted three-body problem with variable masses. *Astrophys Space Sci*. 2010;326:305–314.
- Singh J, Leke O. Equilibrium points and stability in the restricted three-body problem with oblateness and variable masses. *Astrophys Space Sci*. 2012;340:27–41.
- Singh J, Leke O. Effects of oblateness, perturbation, radiation and varying masses on the stability of equilibrium points in the restricted three-body problem. *Astrophys Space Sci*. 2013;340:51–61.
- Veras D, Wyatt MC, Mustill AJ, et al. The great escape: how exoplanets and smaller bodies desert dying stars. *Mon Not R Astron Soc*. 2011;417:2104–2123.
- Letelier PS, Da Silva TA. Solutions to the restricted three-body problem with variable mass. *Astrophys Space Sci*. 2011;332:325–329.
- Leke O, Singh J. Out-of-plane equilibrium points of extra-solar planets in the central binaries PSR B1620–26 and Kepler–16 with clusters of material points and variable masses. *New Astron*. 2023;99:101958.
- Leke O, Celestine M. Zero velocity curves of a dust grain around equilibrium points under effects of radiation, perturbations and variable Kruger 60. *Phys Astron Int J*. 2023;7:280–285.
- Leke O, Orum SA. Motion and zero velocity curves of a dust grain around collinear libration points for the binary IRAS 11472–0800 and G29–38 with a triaxial star and variable masses. *New Astron*. 2024;108:102177.
- Leke O, Cyril-Okeme V, Orum SA. Impact of triaxiality and mass variations on motion around triangular equilibrium points of the restricted three-body problem. *Astron Rep*. 2024;68:1117–1141.
- Leke O, Cyril-Okeme V, Stephen S, et al. Investigation of motion around out-of-plane points in the restricted three-body problem with variable shape and masses. *New Astron*. 2025;114:102311.
- Idrisi MJ. A study of libration in CR3BP under albedo effect. *Int J Adv Astron*. 2017;5:1–6.
- Idrisi MJ, Ullah MS. Restricted three-body problem with albedo effect when the smaller primary is an oblate spheroid. *Glob J Sci Front Res*. 2017;17:9–24.
- Idrisi MJ, Ullah MS. Non-collinear libration in the ER3BP under albedo effects and oblateness. *J Astrophys Astron*. 2018;39:28.
- Singh J, Taura JJ. Motion in the generalized restricted three-body problem. *Astrophys Space Sci*. 2013;343:95–106.
- Singh J, Leke O. Periodic orbits of the Chermnykh-like restricted three-body problem of oblate bodies with radiation. *Astrophys Space Sci*. 2014;350:109–117.
- Singh J, Leke O. Analytic and numerical treatment of motion of dust grain particle around triangular equilibrium points with post-AGB binary star and disc. *Adv Space Res*. 2014;54:1659–1677.
- Jiang IG, Yeh LC. Galaxies with supermassive binary black holes: (I) a possible model for the centers of core galaxies. *Astrophys Space Sci*. 2014;349:881–893.
- Yeh LC, Jiang IG. Galaxies with supermassive binary black holes: (III) The Roche Lobes and Jiang–Yeh Lobe in a core system. *Astrophys Space Sci*. 2016;361:1–13.
- Taura JJ, Leke O. Derivations of the dynamical equations of motion of the R3BP with variable masses and disk. *FUDMA J Sci*. 2022;6:125–133.
- Mestschersky IV. *Works on the Mechanics of Bodies of Variable Mass*. GITTL; 1952:205.
- Yousef S, Kishor R. Effects of the albedo and disc on the zero velocity curves and linear stability of equilibrium points in the generalized restricted three-body problem. *Mon Not R Astron Soc*. 2019;00:1.
- Del Genio A, Way MJ, Kiang NY, et al. Equilibrium Temperatures and Albedos of Habitable Earth-Like Planets in a Coupled Atmosphere–Ocean GCM. NASA; 2017. Accessed May 7, 2025.